INVESTIGATION OF THE MECHANICAL PROPERTIES OF NANOCOMPOSITE SWCNTS/EPOXY BY MICROMECHANICS METHODS AND EXPERIMENTAL WORKS

*H. S. Hedia[1], S. M. Aldousari[2], A. K. Abdellatif[2] and G. S. Abdel Hafeez[2]

[1]King Abdulaziz University, Faculty of Maritime Studies., Jeddah, Saudi Arabia
[2]King Abdulaziz University, Faculty of Eng., Jeddah, Saudi Arabia
*Corresponding Author : Tel. 00966545856959, Fax. 00966 -12-6951805, hassanhedia87@yahoo.com

Abstract

In the present paper, the stiffening effect of carbon nanotubes is quantitatively investigated by micromechanics methods. The Mori-Tanaka effective-field method is employed to calculate the effective elastic moduli of composites with aligned or randomly oriented straight nanotubes. In addition, the epoxy resin is modified experimentally by adding SWCNT with different ratio i.e 0, 0.1, 0.3, 0.5 and 0.7 wt.-%. A comparison between the results for SWCNT/epoxy nanocomposite which obtained analytically and experimentally is done. In the experimental work the epoxy resin is modified by adding SWCNT with different ratios, i.e., 0, 0.1, 0.3, 0.5 and 0.7 wt.-%. The materials are characterized in tension to obtain the mechanical properties of SWCNT/epoxy nanocomposite experimentally. The results of micromechanics methods indicated that the CNTs are highly anisotropic, with Young's modulus in the tube direction two orders of magnitude higher than that normal to the tube. The results shows a nanotube volume fraction of 0.3%of SWCNT improve all mechanical properties such as the tensile strength, modulus of elasticity and the toughness. Avoid the volume fraction greater than 0.5% SWCNT. The optimal value achieved experimentally, (at 0.3% SWCNT) lies between the analytical values (that achieved parallel to the CNT and the randomly orientated straight CNTs).

Keywords: Micromechanics, experimental work, SWCNT, nanocomposite, mechanical properties

1. Introduction

The first step in determining the mechanical properties of Polymer Nano Composite (PNC) is the choice of an appropriate material volume similar to the so-called "representative volume element" (RVE) used in solid mechanics (Fig. 1) Ostoja-Starzewski (2006).
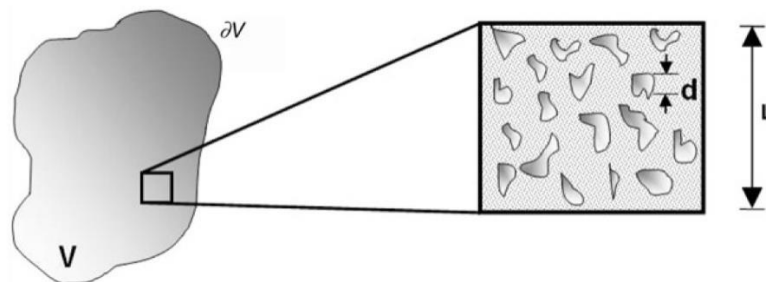
Fig. 1: Representative Volume Element by Ostoja-Starzewski (2006)

Hill (1963) defined the concept of RVE as a part of the solid that is "(a) structurally entirely typical of the whole mixture on average and (b) contains a sufficient number of inclusions for the overall moduli to be effectively independent of the surface values of traction and displacement, so long as these values are macroscopically uniform". Furthermore, Ostoja-Starzewski (2006) proposed a separation of scales technique to define a RVE. These scales are illustrated in Fig. 2 and are (i) the nano-/microscale, d, which is associated with the size of the inclusion, (ii) the mesoscale L, which has the dimensions of the RVE, and (iii) the macroscale, which corresponds to the physical dimensions of the solid. If δ denotes the ratio L/d, then the concept of RVE is defined for $\delta \to \infty$. Hence, for any finite δ the considered volume is not a RVE and, therefore, the determined

mechanical properties depend on the dimensions of the material volume element, creating in this way a sort of scale effect. The proposed method uses the RVE definition by Ostoja-Starzewski (2006) , and the related scale effect to define the material volume defined in Fig. 2.
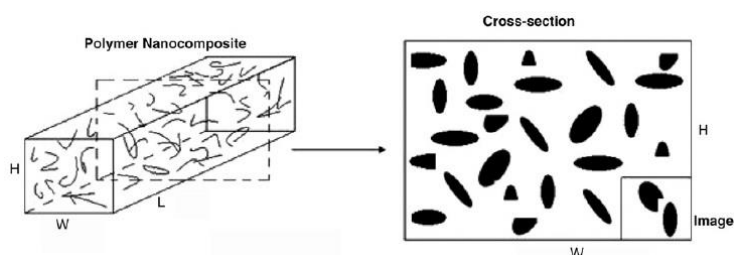
Fig. 2: Proposed material region (MR) for determining mechanical properties of PNC.

The selected MR corresponds to a portion of a cross-section of the actual PNC and coincides with images obtained by microscopy techniques.

This volume is called "material region" (MR) and corresponds to a portion of a cross section of PNC. The advantage of the proposed MR over other candidate volume elements is that it homogenizes the material structure in two different scales: the one defined by the sub-element material structure in each finite element (FE) and the other specified in the overall MR.

Computational modeling and design of materials is becoming increasingly widespread in the development of new advanced material system Panchal et al. (2013). As the properties of materials and the interaction between microstructural phase become increasingly complex, traditional design relying on the experimental Edisonian trial and error approach can become intractable for finding the optimal design. For heterogeneous material, three major factors driving materials properties are phase compositions, geometry and their interaction. To better understand and improve materials behavior, a model is needed to take these statistical microstructure parameters and convert them to the desired properties macroscopic material.

Yi Huang et al. (2007) was investigated the effect of the addition of single-walled carbon nanotubes (SWNTs) to Hysol 9309.2 epoxy using a multi-scale mechanical characterization approach. Effects of SWNTs on the kinetics of epoxy curing were characterized and modeled using macromechanical dynamic mechanical analysis (DMA). Adhesion between SWNTs and microfiber reinforcement was identified with scanning electron microscope (SEM), and effects of SWNTs on mechanical properties of the filled epoxy were quantified using micromechanical tensile testing. Effects of SWNT reinforcement on mechanical behavior of the epoxy matrix were also characterized using nanomechanical characterization. This multi-scale mechanical characterization enabled the effects of SWNTs to be isolated from the epoxy and filler phases inherent in the adhesive.

Harris (2004) states that the Vickers hardness of the polymer was found to increase monotonically with addition of SWNTs up to a factor of 3.5 at 2 wt-% nanotube loading. Greatly enhanced thermal conductivities were also observed. Thus, samples loaded with 1 wt-% unpurified SWNT material showed a 70% increase in thermal conductivity at 40 K, rising to 125% at room temperature. The preparation of SWNT/polyelectrolyte composites by the layer-by-layer method has been described. The films produced in this way were shown to have exceptional mechanical properties. Thus, the average ultimate tensile strength of the films was found to be 220 MPa, with some measurements as high as 325 MPa. This is several orders of magnitude greater than the tensile strength of strong industrial plastics, and indicates that the layer-by-layer method has great promise for the production of strong nanotube-containing composites.

Andrews and Weisenberger (2004) reported that a twofold increase in the tension–tension fatigue strength for an aligned SWNT/epoxy composite was found in comparison to typical carbon fiber/epoxy composites,

In this work, the stiffening effect of carbon nanotubes is quantitatively investigated by micromechanics methods to obtain the modulus of elasticity for the nanocomposite. The results of micromechanics methods are compared to those obtain by the rule-of-mixtures. In addition, an experimental work of SWCNT/Epoxy nanocomposite is done in order to obtain the mechanical properties of it. The results of micromechanics methods are compared to those obtain experimentally.

2. Methodology for Analytical Work

2.1 Using micromechanics methods

2.1.1 Composites reinforced with aligned, straight CNTs.

Consider a linear elastic polymer matrix reinforced by a large number of dispersed CNTs that are aligned, straight and of infinite length. Choose a representative volume element (RVE) V of the composite. The boundary ∂V of the RVE is subjected either to tractions corresponding to a uniform overall stress $\boldsymbol{\sigma}^0$ or to displacements compatible to a prescribed uniform overall strain, $\boldsymbol{\varepsilon}^0$. There are many methods to estimate the overall properties of a composite Hudson (1991). We use the Mori-Tanaka method Mori and Tanaka (1973) in the present study because of its simplicity and accuracy even at a high volume fraction of inclusions.

Mori and Tanaka (1973) assumes that each inclusion is embedded in an infinite pristine matrix subjected to an effective stress $\boldsymbol{\sigma}_m$ or an effective strain $\boldsymbol{\varepsilon}_m$ in the far field, where $\boldsymbol{\sigma}_m$ and $\boldsymbol{\varepsilon}_m$ denote the average stress and the average strain over the matrix, respectively. Thereby, the tensor of effective elastic moduli C of the composite reinforced by aligned inclusions of the same shape is given analytically by

$$\mathbf{C} = (c_m \mathbf{C}_m + c_r \mathbf{C}_r : \mathbf{A}) : (c_m \mathbf{I} + c_r \mathbf{A})^{-1} \tag{1}$$

where, and throughout the paper, a boldface letter stands for a second or fourth-order tensor, and a colon between two tensors denotes contraction (inner product) over two indices; $\mathbf{I}$ is the fourth-order identity tensor; the subscripts m and r stand for the quantities of the matrix and the reinforcing phase, respectively, c_m and c_r denote the volume fractions, and $\mathbf{C}_m$ and $\mathbf{C}_r$ denote the tensors of elastic moduli of the corresponding phases; the fourth order tensor A relates the average strains $\boldsymbol{\varepsilon}_r$ and $\boldsymbol{\varepsilon}_m$ via $\boldsymbol{\varepsilon}_r = \mathbf{A} : \boldsymbol{\varepsilon}_m$ and it is given by

$$\mathbf{A} = [\mathbf{I} + \mathbf{S} : (\mathbf{C}_m)^{-1} : (\mathbf{C}_r - \mathbf{C}_m)]^{-1} \tag{2}$$

where S is the Eshelby tensor which is well documented in Mura's monograph (Mura, 1987).

We consider first a polymer composite reinforced with straight CNTs aligned in the x_2-axis direction. The matrix is assumed to be elastic and isotropic, with Young's modulus E_m and Poisson's ratio $\mathcal{V}_m$. Each straight CNT is modeled as a long fiber with transversely isotropic elastic properties. Therefore, the composite is also transversely isotropic, and its constitutive relation $\boldsymbol{\sigma} = \mathbf{C} : \boldsymbol{\varepsilon}$ can be expressed as

$$\begin{Bmatrix} \sigma_{11} \\ \sigma_{22} \\ \sigma_{33} \\ \sigma_{23} \\ \sigma_{13} \\ \sigma_{12} \end{Bmatrix} = \begin{bmatrix} k+m & l & k-m & 0 & 0 & 0 \\ l & n & l & 0 & 0 & 0 \\ k-m & l & k+m & 0 & 0 & 0 \\ 0 & 0 & 0 & p & 0 & 0 \\ 0 & 0 & 0 & 0 & m & 0 \\ 0 & 0 & 0 & 0 & 0 & p \end{bmatrix} \begin{Bmatrix} \varepsilon_{11} \\ \varepsilon_{22} \\ \varepsilon_{33} \\ 2\varepsilon_{23} \\ 2\varepsilon_{13} \\ 2\varepsilon_{12} \end{Bmatrix} \tag{3}$$

where k, l, m, n, and p are Hill's elastic moduli (Hill, 1965); k is the plane-strain bulk modulus normal to the fiber direction, n is the uniaxial tension modulus in the fiber direction (x_2), l is the associated cross modulus, m and p are the shear moduli in planes normal and parallel to the fiber direction, respectively.

The non-vanishing components of the Eshelby tensor S for a straight, long fiber along the x_2-direction is given by Mura (1987) as:

$$S_{1111} = S_{3333} = \frac{5 - 4\mathcal{V}_m}{8(1 - \mathcal{V}_m)}$$

$$S_{1122} = S_{3322} = \frac{\mathcal{V}_m}{2(1 - \mathcal{V}_m)}$$

$$S_{1133} = S_{3311} = \frac{4\mathcal{V}_m - 1}{8(1 - \mathcal{V}_m)} \tag{4}$$

$$S_{2323} = S_{1212} = \frac{1}{4}$$

$$S_{1313} = \frac{3 - 4\mathcal{V}_m}{8(1 - \mathcal{V}_m)}$$

Fig. 3 shows the effective elastic moduli of a polystyrene composite reinforced by aligned, straight CNTs. The elastic moduli $E_{\parallel}$ and $E_{\perp}$ parallel and normal to CNTs are shown versus the volume fraction c_r of CNTs, where $E_{\parallel}$ and $E_{\perp}$ are related to Hill's elastic moduli by

$$E_{\parallel} = n - \frac{l^2}{k}$$

$$E_{\perp} = \frac{4m(kn - l^2)}{kn - l^2 + mn} \tag{5}$$

2.1.2 Composites reinforced with randomly oriented: straight CNTs.

The effect of randomly oriented, straight CNTs is investigated in this section. The orientation of a straight CNT is characterized by two Euler angles α and β, as shown in Fig. 3. The base vectors $\mathbf{e}_i$ and $\mathbf{e}_i'$ of the global $(o - x_1 x_2 x_3$ and the local coordinate systems $(o - x_1' x_2' x_3')$ are related via the transformation matrix $\mathbf{g}$ Andrews et al. (2002)

$$\mathbf{e}_i = \mathbf{g}_{ij}\mathbf{e}_i' \tag{6}$$

Where $\mathbf{g}$ is given by

$$g = \begin{bmatrix} \cos\beta & -\cos\alpha\sin\beta & \sin\alpha\sin\beta \\ \sin\beta & \cos\alpha\cos\beta & -\sin\alpha\cos\beta \\ 0 & \sin\alpha & \cos\alpha \end{bmatrix} \tag{7}$$

The orientation distribution of CNTs in a composite is characterized by a probability density function $p(\alpha, \beta)$ satisfying the normalization condition

$$\int_0^{2\pi} \int_0^{\pi/2} p(\alpha, \beta) \sin\alpha \, d\alpha \, d\beta = 1 \tag{8}$$

If CNTs are completely randomly oriented, the density function is $p(\alpha, \beta) = 1/2\pi$.

According to the Mori-Tanaka method, the strain $\boldsymbol{\varepsilon}_r(\alpha, \beta)$ and the stress $\boldsymbol{\sigma}_r(\alpha, \beta)$ of the CNT are related to the stress of matrix $\boldsymbol{\sigma}_m$ by
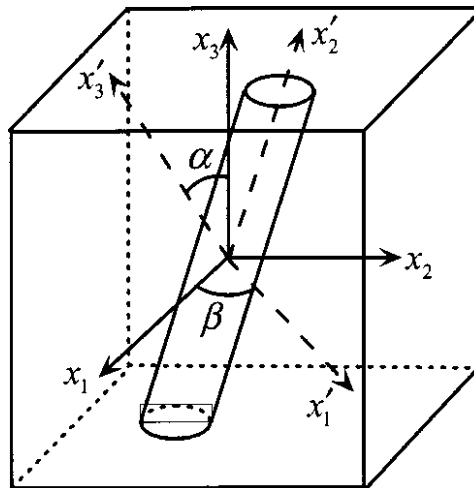
Fig. 3: Effective elastic moduli of a composite reinforced with random aligned straight CNTs

$$\boldsymbol{\varepsilon}_r(\alpha, \beta) = \mathbf{A}(\alpha, \beta) : \boldsymbol{\varepsilon}_m = \mathbf{A}(\alpha, \beta) : \mathbf{C}_m^{-1} : \boldsymbol{\sigma}_m$$

$$\boldsymbol{\sigma}_r(\alpha, \beta) = \mathbf{C}_r : \mathbf{A}(\alpha, \beta) : \boldsymbol{\varepsilon}_m = [\mathbf{C}_r : \mathbf{A}(\alpha, \beta) : \mathbf{C}_m^{-1}] : \boldsymbol{\sigma}_m \tag{9}$$

Where the strain concentration tensor $\mathbf{A}(\alpha, \beta)$ is given by Eq. (2). Then the average strain and stress in all randomly oriented CNTs can be written as:

$$\langle \varepsilon_r \rangle = \left[\int_0^{2\pi} \int_0^{\pi/2} p(\alpha, \beta) \mathbf{A}(\alpha, \beta) \sin \alpha d\alpha \, d\beta \right] : \varepsilon_m$$

$$\langle \sigma_r \rangle = \left[\int_0^{2\pi} \int_0^{\frac{\pi}{2}} p(\alpha, \beta) \left[\mathbf{C}_r : \mathbf{A}(\alpha, \beta) : \mathbf{C}_m^{-1} \right] \sin \alpha d\alpha \, d\beta \right] : \sigma_m \qquad (10)$$

The angle brackets $\langle [\,] \rangle$ represent the average over special orientations. Using the average theorems $\sigma = c_m\sigma_m + c_r\langle\sigma_r\rangle$ and $\varepsilon = c_m\varepsilon_m + c_r\langle\varepsilon_r\rangle$ in conjunction with the effective constitutive relation $\sigma = \mathbf{C}: \varepsilon$, one can get the effective modulus of the composite as

$$\mathbf{C} = (c_m\mathbf{C}_m + c_r\langle\mathbf{C}_r : \mathbf{A}\rangle) : (c_m\mathbf{I} + c_r\langle\mathbf{A}\rangle)^{-1} \qquad (11)$$

When CNTs are completely randomly oriented in the matrix, the composite is then isotropic, and its bulk modulus K and shear modulus G are derived as

$$K = K_m + \frac{c_r(\delta_r - 3K_m\alpha_r)}{3(c_m + c_r\alpha_r)}$$

$$G = G_m + \frac{c_r(\eta_r - 2G_m\beta_r)}{2(c_m + c_r\beta_r)} \qquad (12)$$

K_m and G_m are the bulk and shear moduli of the matrix, respectively. The effective Young's modulus E and Poisson's ratio $\mathcal{V}$ of the composite are given by

$$E = \frac{9KG}{3K + G}$$

$$\mathcal{V} = \frac{3K - 2G}{6K + 2G} \qquad (13)$$

3. Experimental Work

3.1. Materials

The commercial Epoxy resin was a nominally dysfunctional epoxy resin, bisphenol-A glycidol ether epoxy resin (DGEBA). The curing agent was 2-ethyl-4-methylimidazole (EMI-2,4). The epoxy resin and the curing agent as well were obtained from B. D. Classic Enterprizes Inc., Santa FE Springs, CA, USA through an agent in Saudi Arabia.

Five different materials categories are prepared in this work. Details about the constituents of these materials are presented in Tables 1 and 2. The selected percent of SWCNT is 0.0, 0.1, 0.3, 0.5 and 0.7 wt%.

Table 1: Constituents of the control panels (fabricated from neat epoxy)

Test materials	Material abbreviated name	Constituent materials
Neat epoxy	Neat epoxy	Epoxy part A (Resin): Bisphenol-A glycidol ether epoxy resin (DGEBA) Epoxy part B (Hardener): 2-ethyl-4-methylimidazole (EMI-2,4) Viscosity of epoxy (A and B) is 300 cps at 25 ^{o}C.

Table 2: Constituents of SWCNT panels

Test materials	Material abbreviated name	Constituent materials
Single–Wall Carbon Nanotube/Epoxy nanocomposites	SWCNT/E	Epoxy SWCNT: 0.1 wt% (epoxy parts A+B) ◦ Outer diameter = 2 nm ◦ Average length 15 μm ◦ Purity > 98 wt% ◦ Chiralty: Chiral Structure (6,5)

Test materials	Material abbreviated name	Constituent materials
Single–Wall Carbon Nanotube/Epoxy nanocomposites	SWCNT/E	Epoxy SWCNT: 0.3 wt% (epoxy parts A+B) ∘ Outer diameter = 2 nm ∘ Average length 15 μm ∘ Purity > 98 wt% Chiralty: Chiral Structure (6,5)
Single–Wall Carbon Nanotube/Epoxy nanocomposites	SWCNT/E	Epoxy SWCNT: 0.5 wt% (epoxy parts A+B) ∘ Outer diameter = 2 nm ∘ Average length 15 μm ∘ Purity > 98 wt% Chiralty: Chiral Structure (6,5)
Single–Wall Carbon Nanotube/Epoxy nanocomposites	SWCNT/E	Epoxy SWCNT: 0.7 wt% (epoxy parts A+B) ∘ Outer diameter = 2 nm ∘ Average length 15 μm ∘ Purity > 98 wt% Chiralty: Chiral Structure (6,5)

3.1.1. Preparation of neat epoxy panel

Epoxy part A was mixed with epoxy part B and stirred manually for 10 min Kalamkarovl et al. (2002). The hardener (epoxy part B) was added gradually (i.e. drop by drop) while the mixture was being stirred. After stirring the epoxy resin was poured into glass mold that treated by release agent (liquid wax). The mold then procured in an oven for 4 h at a temperature of 40 ^{o}C and post cured by ramping the temperature from 40 ^{o}C to 80 ^{o}C and hold for 2 h Meo and Rossi (2007).

3.1.2. Preparation of nanocomposites

To prepare SWCNTs/Epoxy composite, equal volumes of the two components of the epoxy composite will be used. The suitable amount of the epoxy resin (400 ml) was stirred manually (~40 rpm for 5 minutes) with certain amount of single wall carbon nanotubes (SWCNT) to obtain the target ratio of 0.0, 0.1, 0.3, 0.5 and 0.7 wt% SWCNTs to be sure of the complete mixing as shown in Fig. 4 (A,,B,C,D,E). For this mixture, a suitable amount of the curing agent (400 ml) was added and stirred for 2 min. with the same rpm. The mixture was then sonnicated for other 3 min using a high intensity ultrasonic liquid processor, Cole-Parmer, Inc., USA, Fig. 5.

The mixtures was poured after that on a horizontal surface of the dimensions 28 cm x 70 cm and allowed to cure, which usually takes few minutes. The dispersion of nanofillers is more difficult in a viscous medium, where the viscosity of epoxy increased sharply as the nanofiller loading increased Ehsan and Mokhtar (2012).

The SWCNT composition range was chosen after some experiments showed that in a SWCNT concentration less than 0.1%, the SWCNT was not homogeneously distributed within the sample leading to formation of bad domains in the cured sample as show in in Fig. 6A. Also in case of greater than 0.7% SWCNT (1% SWCNT) concentration there is aggregated domains of SWCNT within the matrix of the epoxy composite sample as show in Fig. 6B.

Due to the fact that sonication parameters can play an important role in enhancement the dispersion of nanofillers in viscous polymers and accordingly the mechanical properties of the nanocomposites, the following sonication parameters are carefully selected based on the literature review Montazeri and Montazeri (2011):

- Sonicator probe with 25 mm diameter was fixed for all the sonication processes.
- Immersion depth of the sonicator probe was fixed at 50 mm, at the center of the container (to avoid the contact between the probe and the container walls), and away about 20 mm from the bottom of the container. Probe immersion depths between (20 to 50 mm) are recommended to prevent the nebulization (formation and release of aerosols) owing to rise of agitation surface.

- The maximum sonication temperature not exceeds 70 ^{o}C. For this purpose, temperature probe tip was fixed at about 1 cm away from the sonicator probe.
- Another important parameter for the ultrasonic dispersion is the sonication amplitude, which is correlated to the power input into the mixture. The maximum sonication amplitude (100%) was applied during the sonication processes. It has been addressed that the best dispersion results are obtained at the highest amplitude of 100%, and hence the highest power input.
- Constant sonication energy (2700 kW.s). The increased viscosity of the epoxy resin due to mixing nanofillers can dampen the cavitations process. Therefore maximum power was used (750 W) for 60 min.
- Operating in pulsed mode with 15 s on and 30 s off. Sonication in pulsed mode retards the rate of temperature increase in the mixture, minimizing unwanted side effects and allowing better temperature control than continuous mode operation.
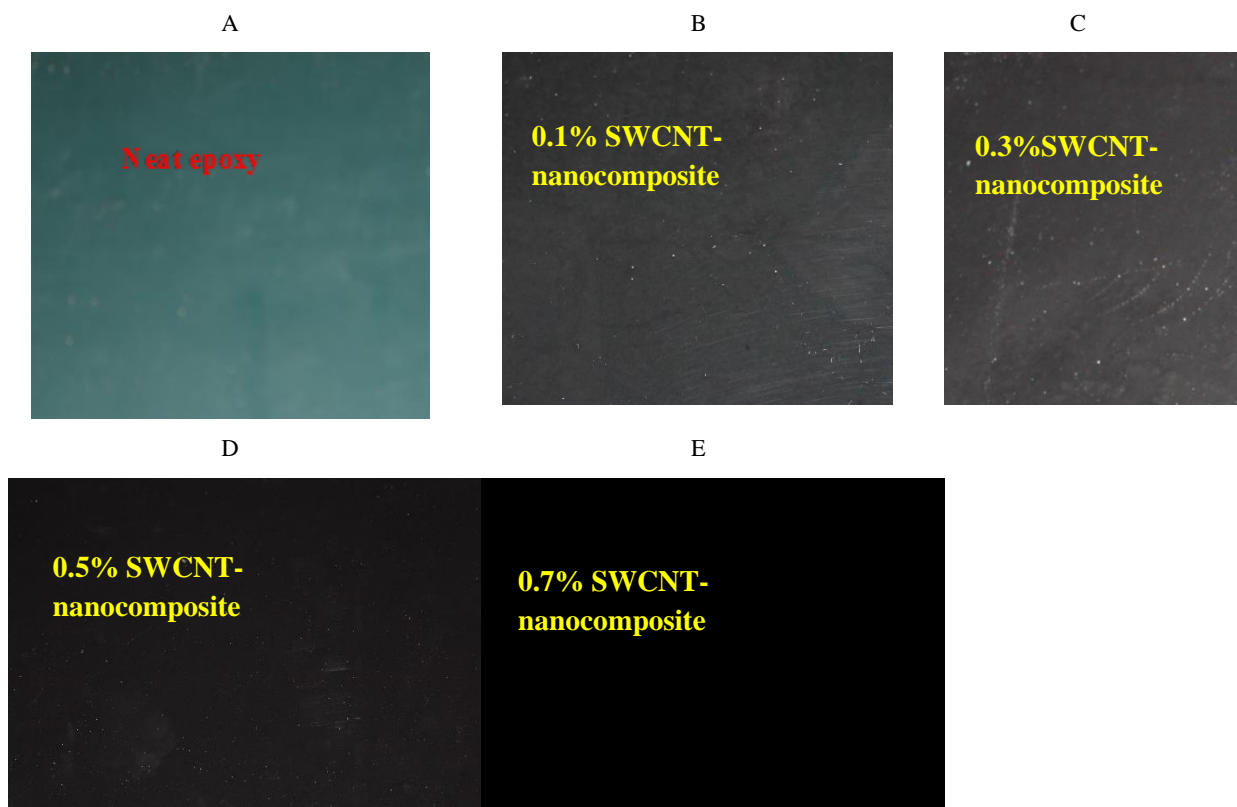
Fig. 4: Photographs of the fabricated neat epoxy and nanocomposites

After sonication, the hardener was added to the epoxy resin and manually stirred for 10 min Kalamkarovl et al. (2002). The nanophased epoxy now is ready to pour into the mold. The nanocomposite panels are prepared and cured by following the same manufacturing procedure of neat epoxy panel.

3.2 Mechanical testing

3.2.1. Tension tests

The test specimens of neat composites and nanocomposites are prepared and tested in accordance with ASTM standard D 638. The test specimens were cut into strips with 165 mm long and 20 mm width. The strips are then machined to the dimensions that illustrated in Fig. 7 and Fig. 8 using milling machine.

4. Results and Discussions

4.1 Analytical Results of micromechanics methods

The Young's modulus and Poisson's ratio of polystyrene are E_m= 1.2 GPa and Poisson's ratio $\mathcal{V}_m$=0.3, respectively. It is noted that CNTs are highly anisotropic, with Young's modulus in the tube direction two

orders of magnitude higher than that normal to the tube. It is observed from Fig. 9 that, because of CNTs' anisotropic property, the elastic modulus $E_{||}$ of the composite in the CNT direction increases much more rapidly with the volume fraction c_r than $E_\perp$ normal to the CNT direction.

Fig. 5: Ultrasonicator used in the preparation of the samples
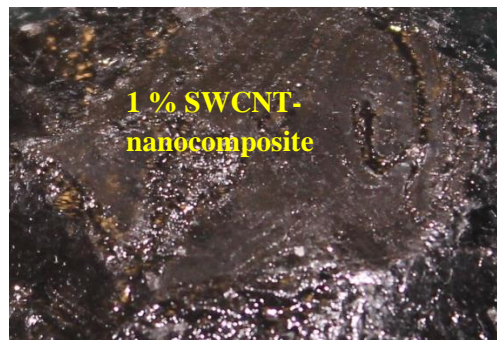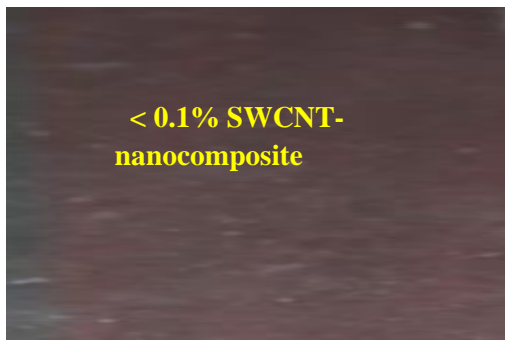
Fig. 6: Photographs of the fabricated neat epoxy and nanocomposites for <0.1% and for 1% of SWNCT
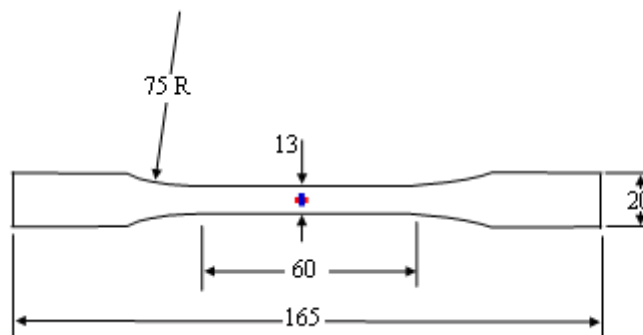
Fig. 7: Dimension of tension test specimens for neat epoxy and nanocomposite
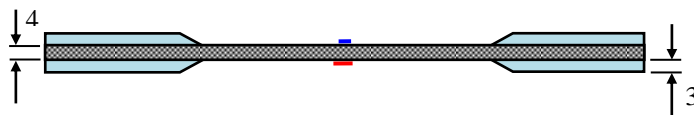
Fig. 8: Dimensions of tension specimens of nanocomposite.
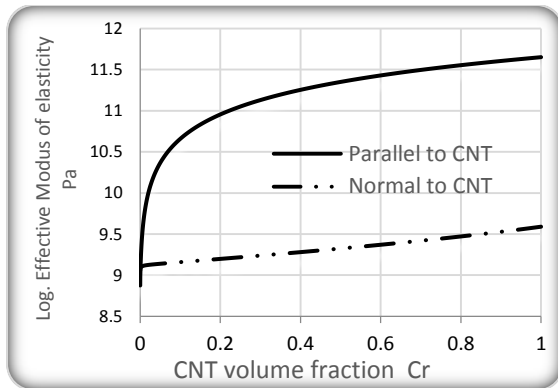
Fig. 9: Relation between effective elastic moduli and the CNT volume fraction
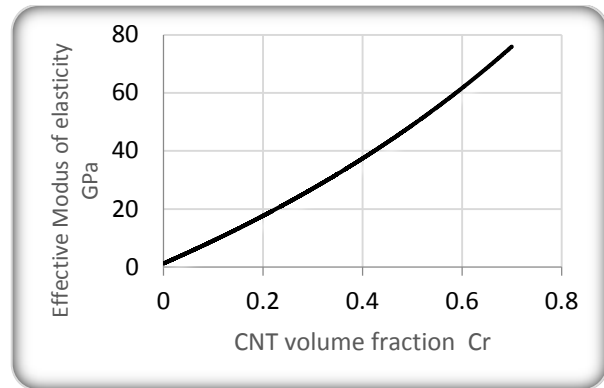
Fig. 10: Effective elastic moduli of a composite reinforced with randomly orientated straight CNTs

Fig. 10 shows the effective Young's modulus versus the volume fraction of randomly oriented, straight CNTs in the same polymer matrix studied in Fig. 9. Young's modulus of the same composite measured by Andrews et al. (2002) is observed to be much smaller than the present theoretical model. Many factors may contribute to this discrepancy, such as the weak bonding between CNTs and matrices, the waviness and agglomeration of CNTs.

4.2 Experimental results

The apparent modulus of neat epoxy is determined from the stress-strain curve of the testing machine as shown in Fig. 11. The value of elastic modulus in the range of 1.2 GPa.

Fig. 12 shows load-displacement diagrams of 0.1, 0.3, 0.5 and 0.7 % SWCNT/epoxy, nanocomposite in tension. It observed that, the tensile strength, modulus of elasticity and the toughness for 0.3% SWCNT/epoxy are higher than those for epoxy and the 0.1, 0.5 and 0.7%SWCNT. The increase of strength and toughness for 0.3% SWCNT/epoxy leads to increase the fracture toughness. However, for 0.7%SWCNT, all-mechanical properties are very bad and the nanocomposite is turned to pure brittle material.

Fig. 13 represents the comparison between the analytical and experimental results of the nanocomposite elastic modulus. The optimal value achieved experimentally, (at 0.3% SWCNT) lies between the analytical values (that achieved parallel to the CNT and the randomly orientated straight CNTs). Many factors may contribute to this discrepancy, such as the weak bonding between CNTs and matrices, the waviness and agglomeration of CNTs.

Table 3 represents the effect of volume fraction on the elastic modulus for nanocomposite. From this table, it is observed that the optimal value of the volume fraction is 0.3% SWCNT. This optimal value produces higher modulus of elasticity for nanocomposite.

Filiou et al. (1992) gives some findings such as (a) fairly isolated filler dispersion and (b) low void content in the matrix, then the deviation of experimental from the conventional rule-of-mixtures or from the micromechanics methods should be mainly due to CNT misalignment and the short length of the individual nanotubes. Other parameters that can affect this deviation are the interface strength and the presence of residual stresses (Filiou et al., 1992). Evidence has already been provided that the fabrication procedure mentioned by Konstantinos et al. (2012) can ensure minimal residual stresses in the composite and that the interface is of reasonable strength as very limited pull-out is observed by Konstantinos et al. (2012). One way to decrease this deviation of CNT forests is to modify chemically the CNT mat to reduce the effective length required for

reinforcement. Possible routes for oxidative treatment of nanotubes is either by washing the as grown mat with an acidic solution (Datsyuk et al., 2008) or by prior plasma treatment.

Table 3: The values of the Modulus of elasticity of nanocomposite as a function of the volume fraction.

Results of Experimental work	
Volume fraction %	Modulus of elasticity GPa
0	1.2
0.1	0.92
0.3	1.62
0.5	1.15
0.7	1.04
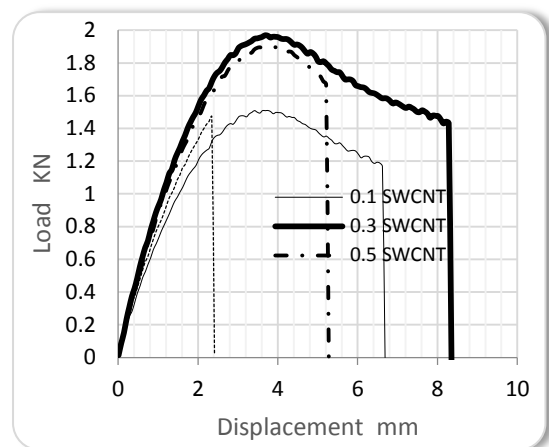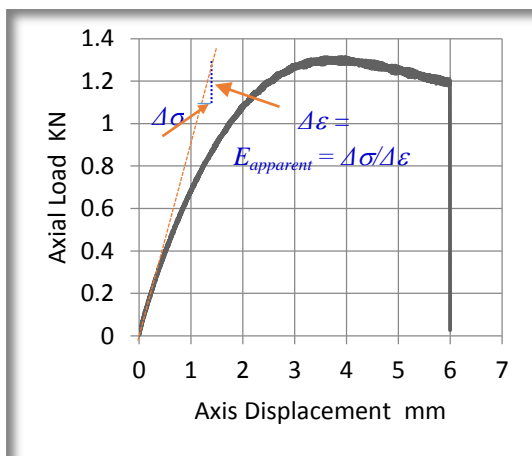
Fig. 11: Load-displacement diagrams of neat epoxy in tension**.**

Fig. 12: Load-displacement diagrams of 0.1, 0.3, 0.5 and 0.7 % SWCNT/E, nanocomposite in tension
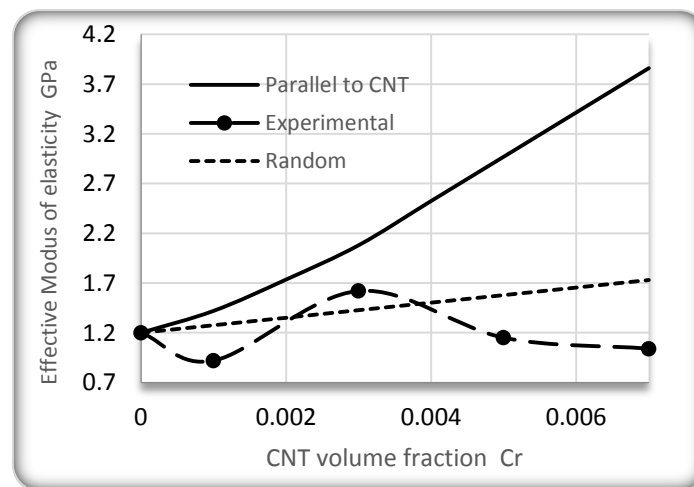
Fig. 13: A comparison between the results of elastic modulus analytically and experimental.

Conclusions

The effect of carbon nanotubes stiffening is quantitatively investigated by micromechanics methods. This method not only provides the relationship between the effective properties and the morphology of carbon nanotube reinforced composites, but also may be useful for improving and tailoring the mechanical properties of nanotube composites.

SWCNTs are highly anisotropic, with Young's modulus in the tube direction two orders of magnitude higher than that normal to the tube. Because of CNTs' anisotropic property, the elastic modulus of the composite parallel to CNT direction increases much more rapidly with the volume fraction c_r than the normal to the CNT direction.

For randomly oriented of SWCNTs, the nanocomposite Young's modulus is much smaller than those for parallel CNTs.

The optimal value achieved experimentally, (at 0.3% SWCNT) lies between the analytical values (that achieved parallel to the CNT and the randomly orientated straight CNTs).

The results show that a nanotube with a 0.3 wt.-% of SWCNT improves all mechanical properties such as the tensile strength, modulus of elasticity and the toughness. However, the increase of strength and toughness for 0.3% SWCNT/epoxy leads to increase the fracture toughness and the lifetime to fracture. A volume fraction greater than 0.5wt.-% of SWCNT produces poor mechanical properties.

Acknowledgements

References

Andrews, R. and Weisenberger, M.C. (2004): Carbon nanotube polymer composites, Current Opinion in Solid State and Materials Science, Vol. 8, pp.31–37, http://dx.doi.org/10.1016/j.cossms.2003.10.006

Andrews, R., Jacques, D., Minot, M., and Rantell, T. (2002): Fabrication of carbon multiwall nanotube/polymer composites by shear mixing, Macromolecular Materials and Engineering, Vol. 287, pp. 395–403.

Datsyuk, V., Kalyva, M., Papagelis, K., Parthenios, J., Tasis, D., Siokou, A., Kallitsis, I. and Galiotis, C. (2008): chemical oxidation of multiwalled carbon nanotubes, Carbon, Vol. 46, No.6, pp. 833–840.

http://dx.doi.org/10.1016/j.carbon.2008.02.012

Ehsan, M. and Mokhtar, A. (2012): A Finite element model to investigate the stress–strain behavior of single walled carbon nanotube, Materials with Complex Behaviour II, Advanced Structured Materials, ,Vol. 16, http://dx.doi.org/10.1007/978-3-642-22700-4_22, Springer-Verlag Berlin Heidelberg

Filiou, C., Galiotis, C. and Batchelder, DN. (1992): Residual-stress distribution in carbon–fiber thermoplastic matrix preimpregnated composite tapes, Composites, Vol. 23, No.1, pp. 28–38.

http://dx.doi.org/10.1016/0010-4361(92)90283-Z

Hill, R. (1965): A self-consistent mechanics of composite materials, Journal of Mechanics and Physics of Solids, Vol. 13, pp. 213–222. http://dx.doi.org/10.1016/0022-5096(65)90010-4

Hill, R. (1963): Elastic properties of reinforced solids: some theoretical principles, Journal of Mechanics and Physics of Solids, Vol.10, pp. 357–372. http://dx.doi.org/10.1016/0022-5096(63)90036-X

Harris, P. J. F. (2004): Carbon nanotube composites, International Materials Reviews, Vol. 49, No. 1, pp. 31-43. http://dx.doi.org/10.1179/095066004225010505

Hudson , J. A. (1991): Overall properties of heterogeneous material , Geophys. J. Int., Vol.107 No.3, pp. 505-511. http://dx.doi.org/ 10.1111/j.1365-246X.1991.tb01411.x

Kalamkarov, A.L., Georgiades, A.V., Rokkam, S.K., Veedu, V.P. and Ghasemi-Nejhad, M.N. (2006): Analytical and numerical techniques to predict carbon nanotubes properties, International Journal of Solids and Structures. ,Vol. 43, pp. 6832–6854. http://dx.doi.org/10.1016/j.ijsolstr.2006.02.009

Konstantinos, G., Dassios, S. M. and Costas, G. (2012): Compressive behavior of MWCNT/epoxy composite mats, Composites Science and Technology, Vol. 72, No.9, pp. 1027–1033. http://dx.doi.org/10.1016/j.compscitech.2012.03.016

Montazeri, A. and Montazeri, N. (2011): Viscoelastic and mechanical properties of multi walled carbon nanotube/epoxy composites with different nanotube content, Materials and Design, Vol. 32, pp. 2301–2307. http://dx.doi.org/10.1016/j.matdes.2010.11.003

Meo, M. and Rossi. (2007): A molecular-mechanics based finite element model for strength prediction of single wall carbon nanotubes, Materials Science and Engineering A, Vol. 454-455, pp. 170-177. http://dx.doi.org/10.1016/j.msea.2006.11.158

Mura, T., (1987): Micromechanics of defects in solids, Martinus Nijhoff Publishers, Dordrecht.

Mori, T., and Tanaka, K. (1973): Average stress in matrix and average elastic energy of materials with misfitting inclusions, Acta Metallurgica ., Vol. 21, pp. 571– 574. http://dx.doi.org/10.1016/0001-6160(73)90064-3

Ostoja-Starzewski, M. (2006): Material spatial randomness from statistical to representative volume element, Probabilistic Engineering Mechanics, Vol. 21, pp. 112–132.

http://dx.doi.org/10.1016/j.probengmech.2005.07.007

Panchal J. H., Kalidindi, S. R., McDowell, D. L. (2013): Key computational modeling issues in integrated computational materials engineering, Journal of Computer-Aided Design, Vol. 45, No. 1, pp. 4-25., http://dx.doi.org/10.1016/j.cad.2012.06.006

Yi Huang, A., Ning, Li A., Yanfeng, Ma. A., Feng, Du. A., Feifei, Li. A., Xiaobo, He. B., Xiao, Lin. B., Hongjun, Gao. B. and Yongsheng, C. (2007): The influence of single-walled carbon nanotube structure on the electromagnetic interference shielding efficiency of its epoxy composites, Carbon, Vol. 45, pp.1614–1621. http://dx.doi.org/10.1016/j.carbon.2007.04.016